AGU PUBLICATIONS

Paleoceanography

RESEARCH ARTICLE
10.1002/2014PA002702

Key Points:
- Foraminiferal I/Ca may be a useful paleoceanographic proxy
- Our I/Ca records demonstrate that OMZs expanded during the PETM

Supporting Information:
- Readme
- Text S1

Correspondence to:
Z. Lu,
zunlilu@syr.edu

Citation:
Zhou, X., E. Thomas, R. E. M. Rickaby, A. M. E. Winguth, and Z. Lu (2014), I/Ca evidence for upper ocean deoxygenation during the PETM, *Paleoceanography*, *29*, 964–975, doi:10.1002/2014PA002702.

Received 17 JUL 2014
Accepted 29 SEP 2014
Accepted article online 1 OCT 2014
Published online 21 OCT 2014

I/Ca evidence for upper ocean deoxygenation during the PETM

Xiaoli Zhou[1], Ellen Thomas[2,3], Rosalind E. M. Rickaby[4], Arne M. E. Winguth[5], and Zunli Lu[1]

[1]Department of Earth Sciences, Syracuse University, Syracuse, New York, USA, [2]Department of Geology and Geophysics, Yale University, New Haven, Connecticut, USA, [3]Department of Earth and Environmental Sciences, Wesleyan University, Middletown, Connecticut, USA, [4]Department of Earth Sciences, University of Oxford, Oxford, UK, [5]Department of Earth and Environmental Sciences, University of Texas, Arlington, Texas, USA

Abstract Anthropogenic global warming affects marine ecosystems in complex ways, and declining ocean oxygenation is a growing concern. Forecasting the geographical and bathymetric extent, rate, and intensity of future deoxygenation and its effects on oceanic biota, however, remains highly challenging because of the complex feedbacks in the Earth-ocean biota system. Information on past global warming events such as the Paleocene-Eocene Thermal Maximum (PETM, ~55.5 Ma), a potential analog for present and future global warming, may help in such forecasting. Documenting past ocean deoxygenation, however, is hampered by the lack of sensitive proxies for past oceanic oxygen levels throughout the water column. As yet no evidence has been presented for pervasive deoxygenation in the upper water column through expansion of oxygen minimum zones (OMZs). We apply a novel proxy for paleoredox conditions, the iodine to calcium ratio (I/Ca) in bulk coarse fraction sediment and planktonic foraminiferal tests from pelagic sites in different oceans, and compared our reconstruction with modeled oxygen levels. The reconstructed iodate gradients indicate that deoxygenation occurred in the upper water column in the Atlantic, Indian Oceans, and possibly the Pacific Ocean, as well during the PETM, due to vertical and potentially lateral expansion of OMZs.

1. Introduction

Global warming reportedly leads to deoxygenation in the modern and future oceans [*Helm et al.*, 2011]. With present global warming, OMZs are shoaling worldwide [*Whitney et al.*, 2007; *Bograd et al.*, 2008; *Gilly et al.*, 2013], strongly impacting the structure of pelagic ecosystems [*Stramma et al.*, 2012]. It is important to predict future oceanic oxygen levels because of the consequences of decreased oxygen levels for marine life (including fisheries) [*Keeling et al.*, 2010; *Falkowski et al.*, 2011]. The geological record of past global warming episodes may be used to obtain information on the extent and severity of oceanic deoxygenation and its effects on marine biota [*Reid et al.*, 2009], as has been done for ocean acidification [*Hoenisch et al.*, 2012].

Reconstruction of global oceanic oxygen levels of the past is difficult, however. Trace elements and isotopic proxies measured on bulk sediment reflect local to regional oxygen conditions in bottom or pore waters, or potentially the relative area of the global sea floor affected by anoxia/hypoxia [*Algeo and Lyons*, 2006; *Anbar and Gordon*, 2008]. In the present oceans, we see low-oxygen conditions in semienclosed, poorly ventilated basins such as the Black Sea, but the largest oceanic regions with anoxic-dysoxic waters are the oxygen minimum zones (OMZs), midwater regions with O_2 concentrations $<$0.5 ml/L that intercept continental margins generally at bathyal depths (200–1000 m) [*Levin*, 2003; *Gooday et al.*, 2010]. Modern OMZs are well developed in the high-productivity regions of the eastern Pacific Ocean, the Arabian Sea, and the Bay of Bengal [*Levin*, 2003]. Below OMZs, bottom waters may well be oxygenated: the eastern equatorial Pacific OMZ, for instance, has its minimum oxygen levels between 200 and 700 m in a region where the water depth is more than 4000 m [*Gilly et al.*, 2013].

The geological record contains examples of oceanic deoxygenation during rapid global warming episodes of the past, such as the Mesozoic Oceanic Anoxic Events (OAEs) [*Jenkyns*, 2010]. The Paleocene-Eocene Thermal Maximum (PETM, ~55.5 Ma) has been considered a less intense counterpart of the OAEs [*Jenkyns*, 2010] and our best analog for future global warming [*Hoenisch et al.*, 2012]. More complete global records can be constructed for this younger event than for Mesozoic events [*McInerney and Wing*, 2011; *Dunkley Jones et al.*, 2013]. Laminated, organic-rich shales, as typical for OAEs, were deposited during the PETM in marginal basins in the Tethys [*Speijer and Wagner*, 2002], Peri-Tethys [*Gavrilov et al.*, 1997; *Dickson et al.*, 2014], and in the Arctic

Ocean [*Moran et al.*, 2006; *Stein et al.*, 2006]. Decreased bioturbation indicates lowered oxygen levels along continental margins in New Zealand [*Nicolo et al.*, 2010] but is not associated with benthic foraminiferal assemblages indicative of low-oxygen levels [*Alegret et al.*, 2009, 2010]. Along the New Jersey shelf, oxygen levels declined, but anoxia was not reached [*Stassen et al.*, 2012]. Low-oxygen conditions occurred in the semirestricted Arctic before, during, and after the PETM [*Sluijs et al.*, 2006], as well as in its marginal basins [*Akhmet'ev et al.*, 2010; *McNeil et al.*, 2013; *Nagy et al.*, 2013]. The widespread anoxic to hypoxic conditions in marginal basins have been linked to eutrophication (New Jersey [*Gibbs et al.*, 2006; *Stassen et al.*, 2012]), possibly due to increased nutrient inputs as supplied by a more active hydrological cycle during the extreme warmth of the PETM [*Ravizza et al.*, 2001; *Wieczorek et al.*, 2013].

Globally, oxygen levels in open ocean basins may have dropped slightly during the late PETM, as argued from Mo-isotope evidence [*Dickson et al.*, 2012] and from modeling [*Winguth et al.*, 2012]. Sediment chemical evidence suggests that bottom waters were suboxic at abyssal to bathyal depths in the Atlantic and Southern Oceans across the PETM with intensification during the event but not in the Pacific [*Chun et al.*, 2010; *Paelike et al.*, 2014], and there is no evidence for global bottom water anoxia during the peak of the PETM [*Thomas*, 2007].

In contrast to marginal basins, suboxic conditions in open oceans have not been linked to eutrophication: warming, changes in ocean stratification circulation, and oxidation of methane hydrates have been invoked as causes for suboxia [*Paelike et al.*, 2014]. Site-specific reconstruction of paleoredox conditions at surface water and midwater depths cannot be performed using traditional proxies, unless full euxinia occurs within the photic zone and the organic biomarker isorenieretane can be used [*Summons and Powell*, 1987; *Koopmans et al.*, 1996].

We use the novel proxy I/Ca in the first attempt to reconstruct paleo-oxygenation levels in the upper ocean [*Lu et al.*, 2010; *Hardisty et al.*, 2014]. The I/Ca in marine bulk carbonate is sensitive to relatively subtle redox changes. We use I/Ca in bulk coarse fraction carbonate (dominantly planktonic foraminifera) and in monogeneric planktonic foraminiferal tests to investigate potential changes in the oxygenation state of mixed-layer and thermocline ocean waters during the PETM. Deriving a fully quantitative relationship between dissolved oxygen and foraminiferal I/Ca is beyond the scope of this work, because there are currently no cultivation studies of planktonic foraminifera and no core top I/Ca studies paired with water column iodine speciation analyses for the modern ocean. Therefore, our inferences from I/Ca remain qualitative. Our main goal is to test the potential of I/Ca in foraminifera as a paleoceanographic proxy for oxygenation changes at multiple open ocean locations. We assess various factors that might complicate the use of this proxy and demonstrate the potential of I/Ca to reflect past deoxygenation through agreement with model simulations of oxygenation levels [*Winguth et al.*, 2012].

2. Iodine in Seawater and Foraminifera

2.1. Marine Chemistry of Iodine

The I/Ca proxy is based on knowledge of iodine speciation in the modern oceans. In modern seawater, the total iodine content, the sum of iodate and iodide concentrations, is invariant at around 0.45 μmol/L [*Kuepper et al.*, 2011]. In the upper ocean, the iodate concentration is inversely correlated to the iodide concentration. Iodate as a micronutrient is used by marine organisms [*Kuepper et al.*, 2011]. High primary productivity and decomposition of organic matter may cause up to ~50% iodate loss in surface ocean waters, and iodide production deeper in the water column, as observed at many locations including Hawaii and Bermuda [*Campos et al.*, 1996], the Weddell Sea [*Campos et al.*, 1999; *Bluhm et al.*, 2011], the Mediterranean Sea [*Tian et al.*, 1996], the Arabian Sea [*Farrenkopf and Luther*, 2002], and Antarctic coastal waters [*Chance et al.*, 2010].

In addition to the biologic uptake/release, iodine speciation is also strongly affected by redox conditions. Under hypoxic conditions, more than 75% of iodate is converted to iodide [*Truesdale and Bailey*, 2000], and iodide is the dominant species below the oxygenated surface water in anoxic basins [*Wong and Brewer*, 1977]. Iodine occurs mostly as iodate in oxic bottom waters, and upwelling of oxygenated deep water may compensate for iodate reduction in surface waters [*Truesdale and Bailey*, 2002].

The vertical iodate concentration profile is thus influenced by productivity and the presence/absence of an oxygen minimum zone (OMZ). If there is no OMZ (Figure 1a), the iodate concentration increases downward

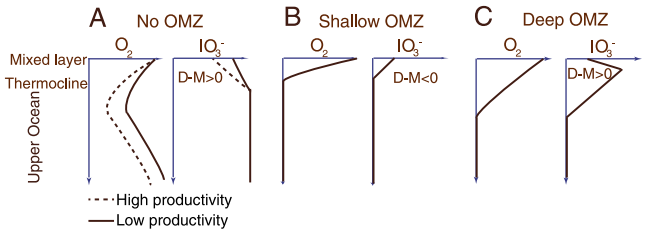

Figure 1. (a–c) Schematic seawater iodate and oxygen concentration profiles. D-M stands for the difference between I/Ca of deep (*Subbotina*) and mixed-layer (*Acarinina*, *Morozovella*) calcifiers.

from the mixed layer, where primary productivity occurs, to greater depths [*Jickells et al.*, 1988]. O_2 generally decreases with depth due to respiration, but iodate is not used as an oxidant before complete O_2 consumption, and its concentration increases to the whole-ocean value. In contrast, when there is an OMZ at relatively shallow levels (Figure 1b), the iodate concentration decreases from the mixed layer down to the upper OMZ [*Smith et al.*, 1990]. When the OMZ is located deeper in the water column (Figure 1c), the iodate concentration increases from the mixed layer downward, then decreases to zero in the OMZ [*Rue et al.*, 1997].

2.2. Water Column Depth Gradient in Planktonic Foraminiferal I/Ca

Primary productivity and oxygen levels act as first-order controls on the iodate concentration in ocean waters; thus, they should be the dominant control of I/Ca in planktonic foraminiferal tests. We thus expect I/Ca to be lower in mixed-layer dwelling planktonic foraminifera at higher productivity (Figure 1a). Oxygen levels are generally positively correlated to seawater iodate concentrations, thus I/Ca in foraminifera. The development of OMZs, particularly the shallow ones, should cause an overall decrease in planktonic foraminiferal I/Ca, with lower values in thermocline calcifiers (D) than in mixed-layer calcifiers (M) (Figure 1).

Changes in I/Ca can be anticipated for simple scenarios in which productivity and oxygen levels vary simultaneously. A combination of increased productivity and deoxygenation should lead to sharply lower I/Ca in planktonic foraminifera, with these two factors working in the same direction. In contrast, the net effect of decreased productivity and deoxygenation (as potentially caused by increased ocean stratification) depends on the relative magnitude of the changes, because they have opposite effects. Changes in I/Ca in mixed-layer (M) compared to I/Ca in deep-dwelling (D) planktonic foraminifera thus reflect changes in the iodate depth gradient, related to productivity and the vertical extent of OMZs (Figure 1).

3. Methods

3.1. Samples, Sites, and Age Models

We used bulk coarse fraction samples (BCF, >63 μm) and single genus planktonic foraminiferal tests, targeting the redox conditions above and within the thermocline, broadly named upper ocean waters. The BCF consists dominantly of planktonic foraminiferal tests calcified in upper ocean waters [*Ezard et al.*, 2011]. We picked three planktonic genera, mixed-layer calcifiers *Acarinina* spp. and *Morozovella* spp. (M), and deep calcifier *Subbotina* spp. (D) [*Ezard et al.*, 2011], and calculated the difference in I/Ca between D and M (D-M). For some pre-CIE (carbon isotope excursion) samples from Sites 1262 and 865, we sieved BCF samples in eight size fractions from 63 to >250 μm and analyzed these separately for I/Ca.

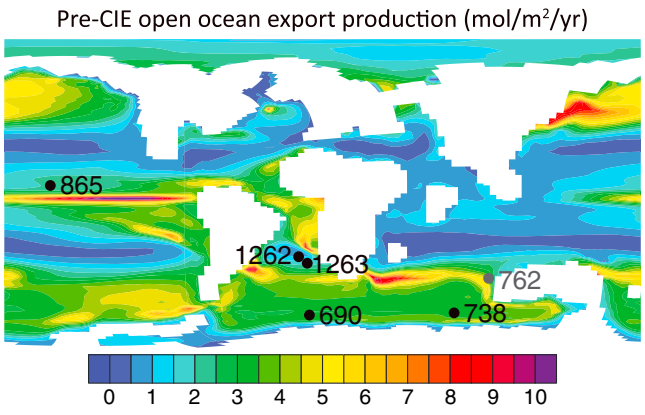

Figure 2. Studied sites plotted on a paleomap of the modeled export productivity during the late Paleocene [*Winguth et al.*, 2012].

We focused on well-studied open ocean sites in the Pacific (Site 865), Southeast Atlantic Walvis Ridge (Sites 1262 and 1263), Southern Ocean Weddell Sea (Site 690), and Indian Ocean (Site 738) (Figure 2). A few samples from Site 762 (Indian Ocean) were analyzed to compare with modeled productivity. Age models are based on correlation through carbon isotope records [*Zachos et al.*, 2005], with numerical ages relative to the base of the carbon isotope excursion (CIE)

during the PETM for Sites 690, 1262, and 1263 as in *Röhl et al.* [2007], for Site 738 as in *Larrasoana et al.* [2012], and for Site 865 as in *Penman et al.* [2014]. The age model for Site 762 is poorly constrained and is based on the bulk stable isotope record in *Thomas et al.* [1992]. To constrain background I/Ca, we extended the records to 1–2 Myr into the Paleocene before the onset of the carbon isotope excursion (CIE).

3.2. Cleaning Procedures

For each sample, 3–5 mg of coarse fraction material was weighed, crushed, and rinsed with deionized water to remove residual pore water before dissolution and not further cleaned by oxidative or reductive reagents. The single genus planktonic tests were picked and then cleaned using the procedure following the Mg/Ca protocol [*Barker et al.*, 2003]. The shells were gently crushed between two clean glass slides to open the chambers. After clay removal in an ultrasonic water bath, NaOH-buffered H_2O_2 solutions were added to the samples, which were then heated in boiling water for 20 min. Carbonate materials were then thoroughly rinsed. We did not use reductive cleaning, because contribution of iodine from Mn oxides is negligible (see below).

3.3. Inductively Coupled Plasma Mass Spectrometry Measurements

I/Ca was measured on a quadrupole inductively coupled plasma mass spectrometry (Bruker M90) at Syracuse University. After cleaning, carbonate samples were dissolved in 3% nitric acid and diluted to form solutions with ~50 ppm Ca for analyses. Fresh calibration standards, matching the sample matrix, were prepared for every batch of samples. The sensitivity of iodine is tuned to about 80–120 kHz for 1 ppb standard, and the standard deviation for three blanks in a row is ~0.3 kHz. The precision of ^{127}I is typically better than 1% and is not reported separately for each sample. The long-term accuracy is guaranteed by frequent repeats of the reference material JCp-1 [*Lu et al.*, 2010]. The detection limit of I/Ca is typically below 0.1 μmol/mol.

3.4. Partial Dissolution, Mn Oxide Coatings, and Temperature

To test the potential influence of postdepositional partial dissolution of shell carbonate on I/Ca, 200–250 tests of *Acarinina* spp. and *Morozovella* spp. were picked from Paleocene samples. They were crushed, homogenized, and divided into six subsamples. Two were not acidified, and the others were soaked in 0.1 ml of 0.08 N HNO_3 for 3 min, repeated up to 4 times. After partial dissolution, the tests were cleaned as normal samples and dissolved for measurement.

To evaluate potential contamination of I from Mn oxides, we determined the temporal trend in I/Ca after reductive cleaning [*Boyle and Keigwin*, 1985] in six coarse fraction samples from between 100 and 150 kyr after the onset of the CIE at Site 1262; 2–4 mg of micronodules were separated from carbonate material by picking then treated the same as bulk coarse fraction samples for detecting any oxides associated iodine signal.

To evaluate temperature dependence of the iodate partition coefficient, calcite crystals were synthesized in deionized water by mixing $CaCl_2$ and Na_2CO_3 solutions at three different temperatures (6, 19, and 33°C). Crystals grew in a refrigerated or heated water bath over a period of 2 weeks, reaching a size of ~0.3 mm. The calcite was thoroughly rinsed before dissolution for I/Ca analysis.

4. Results

The general patterns in BCF and single genus records are similar at Sites 865 and 690 (Figure 3), although I/Ca values are higher at Site 865 throughout the records. At both sites, the I/Ca values in deep-dwelling planktonic foraminifera (D) are higher than those in mixed-layer dwelling foraminifera, resulting in D-M values that are generally >0 (Figure 4), increasing during the PETM. At both sites, the I/Ca in monogeneric records dropped at the start of the CIE. At Site 865, the BCF record also shows a decrease; at Site 690 such a decrease may exist, but our data do not cover the peak CIE. At this site, two samples in the peak PETM (<25 kyr) show a much larger decline in I/Ca in M than in D so that the D-M reaches a maximum (~2 μmol/mol, Figure 4).

At Site 1262, the BCF and monogeneric I/Ca values are even higher than at Site 865 and decrease during the CIE (Figure 3). At this site, however, there are no clear and consistent offsets between I/Ca in D and M, and D-M is generally negative, with a few positive points ~100 kyr after the start of the CIE (Figure 4). In the Paleocene, I/Ca values in BCF are significantly higher than those in all monogeneric records. In two Paleocene samples from Site 1262, the I/Ca values of the <125 μm size fraction are considerably higher than

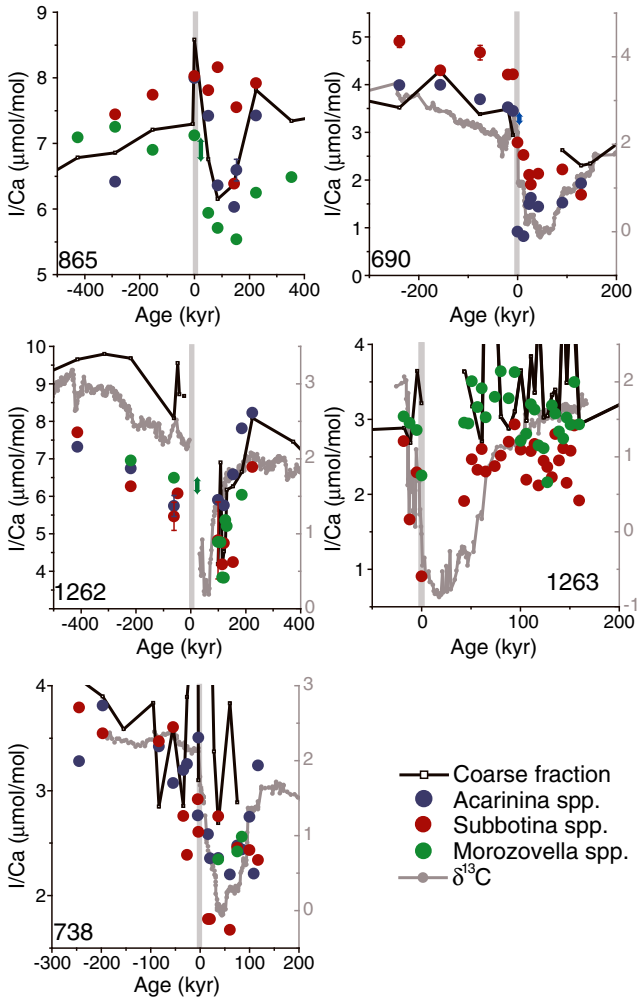

Figure 3. Coarse fraction and single genus I/Ca for open ocean sites. Error bars show standard deviations of repeated measurements on picked and cleaned shells. The colored double-headed arrows (green for Sites 865 and 1262 and blue for Site 690) next to the grey bar mark the potential I/Ca decrease caused by the warming-induced changes in the partition coefficient [*Dunkley Jones et al.*, 2013]. Bulk carbon isotope data for Sites 1262 and 1263 [*Zachos et al.*, 2005], Site 690 [*Bains et al.*, 1999], and Site 738 [*Larrasoana et al.*, 2012].

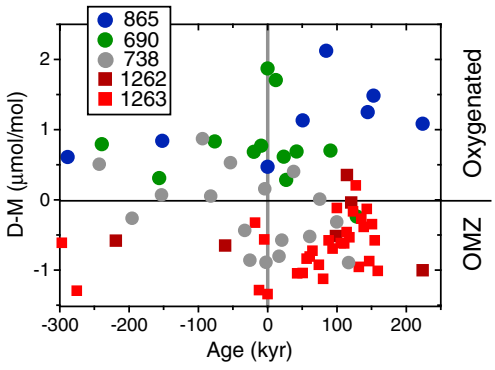

Figure 4. Differences in I/Ca between the deep (D) and mixed-layer (M) calcifiers for each site, indicating local iodate gradient and oxygenation.

those in larger size fractions (Figure 5), in contrast to a coeval sample from Site 865, where values do not change with size. Site 1262 was at a paleodepth of ~3400 m [*Zachos et al.*, 2005], i.e., close to the carbonate compensation depth and possibly below the lysocline at that time, and carbonate dissolution (even before the PETM) could have led to preferential dissolution of planktonic over benthic foraminifera [*Nguyen et al.*, 2009]. Visual inspection of these samples showed that benthic foraminifera are indeed dominant in the smaller size fractions. Iodate in oxic bottom waters is much higher than in surface waters (Figure 1), and these high values in BCF as compared to the monogeneric planktonic records reflect the common presence of benthic foraminifera in BCF at Site 1262 (Figure 3).

At Site 1263, close to Site 1262 but at a paleodepth of ~1500 m [*Zachos et al.*, 2005], the BCF record shows large, random fluctuations during the PETM, possibly also due to preferential dissolution of planktonic foraminifera and a higher benthic/planktonic ratio in BCF. Overall, the values of monogeneric M (*Morozovella* spp.) were higher than those of D (*Subbotina* spp.), leading to overall negative D-M (Figure 4), with the exception of a few positive data points, coeval with those at Site 1262, ~100 kyr after the onset of the CIE. D-M may have decreased at the onset of the CIE.

The record at Site 738 is similar to that at Site 1263, with large fluctuations in the I/Ca in the BCF record during the PETM. At this site, however, there is no clear, consistent offset between D and M I/Ca values, and the monogeneric records show a decrease in I/Ca during the PETM. D-M values fluctuate and are relatively higher in the Paleocene and relatively lower within about 100 kyr after the onset of the CIE.

The effects of dissolution and Mn oxide coatings on I/Ca signal are found to be minimal and are not further discussed. The partition coefficient of iodate decreases at higher temperatures for

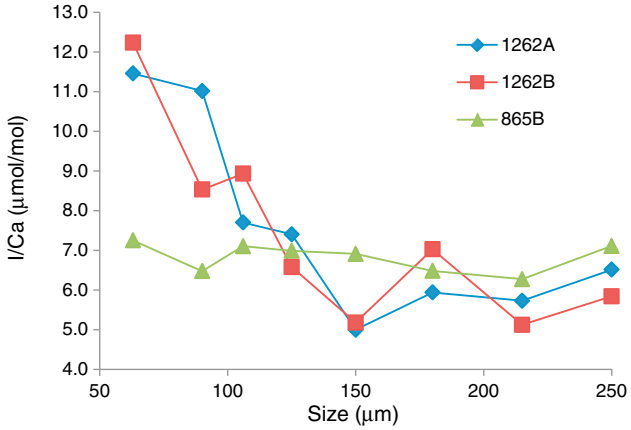

Figure 5. I/Ca values in different size fractions of bulk coarse fraction in samples from Sites 1262 and 865.

the synthetic calcite. The potential contribution of PETM warming to I/Ca changes in the records are estimated using the synthetic calcite data, and experimental results are shown in the supporting information.

5. Discussion

5.1. Pre-PETM Productivity Versus I/Ca

The Paleocene I/Ca values in the monogeneric records differ substantially between sites (Figure 3), with values at Sites 690, 1263, and 738 generally lower (values 2–4 μmol/mol) and Sites 865 and 1262 higher (6–8, Figure 3). We expect planktonic I/Ca to reflect paleoproductivity when there is no overriding effect of oxygenation levels, with lower I/Ca at higher productivity [*Chance et al.*, 2010] (Figure 1a). In order to test whether the differences in I/Ca in our planktonic foraminiferal tests from different sites could be related to differences in productivity, we compared the average I/Ca in mixed-layer planktonic (*Acarinina* spp.) with the export productivity modeled for these sites in Community Climate System Model Version 3 (CCSM3) [*Winguth et al.*, 2012] (Figures 2 and 6). The patterns in Paleocene modeled productivity generally resemble present-day patterns of export production [*Doney et al.*, 2006].

The modeled productivity and I/Ca in planktonic foraminifera are negatively correlated as predicted (Figure 6). Modeling and the I/Ca data indicate that Sites 1262 and 865 had relatively low productivity compared to Sites 690, 738, and 762. Microfossil evidence agrees with the hypothesis that productivity was lower at Site 865 than at Site 690 [*Bralower et al.*, 1995]. Site 762 (Indian Ocean) had somewhat higher productivity than at Sites 738 (Indian Ocean) and 690 (Weddell Sea). Productivity thus may have been one of the dominant controls on iodate concentrations in the upper oceans during the Paleocene, as in modern oceans.

5.2. Productivity Changes During the PETM

Because productivity and oxygenation changes are often intertwined, the interpretation of I/Ca as a paleoredox signal requires a thorough review of productivity changes during the PETM. It is not clear how primary and export production in the open ocean changed during the PETM, and changes may not have been globally uniform [*Winguth et al.*, 2012]. At many sites, there is conflicting evidence on productivity, e.g., decreasing productivity inferred from nannofossil assemblages at Weddell Sea Site 690 [*Bralower*, 2002], but potentially short-term increasing productivity from Sr/Ca in nannofossils at the same site [*Stoll et al.*, 2007].

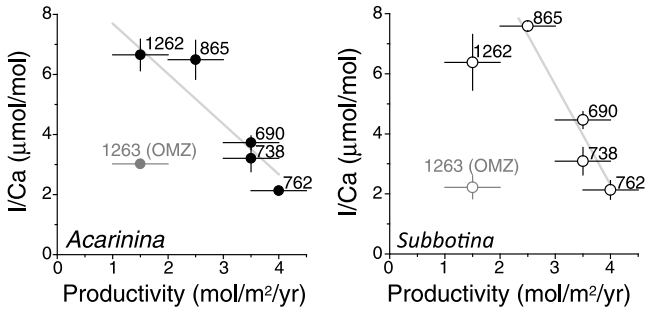

Figure 6. Average values and standard deviations of I/Ca in late Paleocene mixed-layer and deep-dwelling calcifiers, correlated with the modeled productivity in *Winguth et al.* [2012]. *Morozovella* was used instead of *Acarinina* for Site 865 due to the lack of shells. Site 1263 falls off the trend and is related to a shallow OMZ.

On a global scale, primary productivity may have decreased in vast open ocean areas [*Gibbs et al.*, 2006; *Paytan et al.*, 2007; *Thomas*, 2007; *Winguth et al.*, 2012; *Norris et al.*, 2013] and remained close to be constant in other regions [*Stoll et al.*, 2007; *Gibbs et al.*, 2010]. The trophic resource continuum may have expanded so that globally more extreme oligotrophic as well as eutrophic conditions occurred [*Hallock*, 1987; *Boersma et al.*, 1998].

5.3. PETM Open Ocean Deoxygenation

Records from the open ocean Pacific (865), Weddell Sea (690), SE Atlantic (1262 and 1263), and Indian (738) sites,

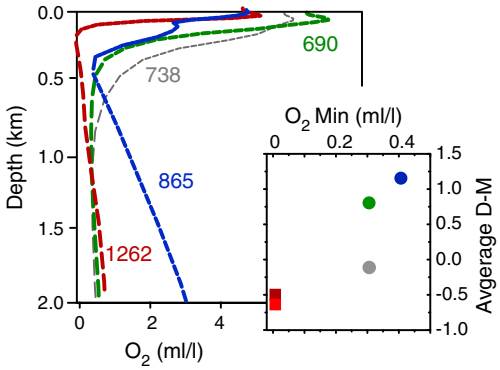

Figure 7. O_2 profiles simulated in CCSM3 model under 4xCO_2 conditions [*Winguth et al.*, 2012]. Insert compares the average D-M values for the studied interval (from −300 kyr to 250 kyr relative to the onset of the PETM) with the modeled minimum O_2 concentration at each site.

although not yet at high resolution, generally show decreased I/Ca in monogeneric mixed-layer and thermocline dwelling planktonic foraminiferal records over the CIE (Figure 3), with minimum values around the peak CIE. Such a decrease in I/Ca likely indicates widespread deoxygenation in the upper ocean, since neither microfossil records [*Kelly et al.*, 1996; *Bralower*, 2002; *Gibbs et al.*, 2006] nor modeling [*Winguth et al.*, 2012] support widespread increased pelagic productivity during the PETM. The decrease in I/Ca at Site 690 is very large, dropping to values of ~1 μmol/mol (Figure 3) and probably cannot be explained by productivity spikes as indicated by barite accumulation rates [*Ma et al.*, 2014] (Figure 6). Data on magnetotactic bacteria suggest Fe dust-induced increased productivity at Site 738 [*Larrasoana et al.*, 2012], but there is only one data point for the barite proxy [*Ma et al.*, 2014]. Productivity declined at nearby Site 1135 according to nannofossil evidence [*Jiang and Wise*, 2009].

The I/Ca decrease at Site 865 is relatively small, which may be explained by increased productivity instead of deoxygenation, but microfossil evidence strongly indicates a decrease in productivity [*Kelly et al.*, 1996; *Kelly*, 2002]. There is some evidence for increased productivity during the PETM at Site 690 [*Stoll and Bains*, 2003], but this is controversial [*Bralower et al.*, 2004; *Stoll et al.*, 2007]. Barite accumulation rates somewhat increased at several Pacific Sites but that might indicate increased remineralization and not increased primary productivity [*Ma et al.*, 2014]. Therefore, we suggest that Site 865 went through mild deoxygenation during the PETM, a condition possibly typical for oligotrophic parts of the Pacific Ocean.

We thus interpret the observed general decrease in I/Ca at the onset of the PETM as most probably indicative of widespread deoxygenation in the upper ocean waters. Ocean stratification induced by warming may be the mechanism for lowering oxygen levels [*Norris et al.*, 2013], and the elevated respiration rates at higher temperatures may also play a role [*John et al.*, 2013]. The deoxygenation likely was stronger in the Atlantic and Indian Oceans than in the Pacific Ocean in agreement with geochemical evidence [*Paelike et al.*, 2014], possibly due to increased stratification.

5.4. Iodate Gradients and OMZs

We next use the difference in I/Ca values of deep dwellers and mixed-layer dwellers (D-M) to reconstruct iodate gradients and detect whether an OMZ was present and then compare the results with dissolved oxygen profiles modeled with CCSM3 at 4xCO_2 (Figures 1, 4, and 7) [*Winguth et al.*, 2012]. The average D-M through the studied interval is positively correlated with the minimum oxygen levels in the water column estimated from the model (insert in Figure 7). Qualitatively, the ranking of oxygen levels among these sites is comparable in proxy data versus model output, although absolute values of dissolved oxygen cannot be derived until the proxy is quantitatively calibrated.

Sites 865 and 690 have predominantly positive D-M values before, during, and after the PETM, indicating that no strong OMZ was present or it was deep (Figure 1c). We argued above that deoxygenation occurred at Sites 690 and 865 during the PETM, especially for the very low I/Ca at Site 690, but the D-M values remained positive at both sites. This could be explained through comparison with the iodate profile in modern OMZs (Figures 1a and 1c). The iodate concentrations may increase from the surface to near the upper boundary of the OMZ, then drop rapidly to zero within the OMZ [*Rue et al.*, 1997]. If Sites 690 and 865 had normal open ocean iodate profiles in the Paleocene and then switched to OMZ-type iodate profiles during the PETM, I/Ca of both deep (D) and mixed-layer (M) genera would have decreased while maintaining positive D-M values, as long as the deeper dwellers lived above the iodate reversal around the upper boundary of OMZ.

Monogeneric records show declining I/Ca at the onset of the PETM at Site 738. D-M values varied around zero due to the lack of a clear difference between D and M values. Potentially, an OMZ was present throughout the studied interval. The OMZ might have been deeper before the PETM, corresponding to mostly positive D-M values, and then shoaled across the onset of the PETM as indicated by a change to largely negative D-M values (Figure 4).

Sites 1262 and 1263, on a depth transect along Walvis Ridge, have negative D-M values in most samples, indicative of OMZ presence throughout the studied interval. Exceptions are a few positive values at about 125 kyr after the onset of the CIE at both sites (Figure 4). Bulk sediment Mn and U enrichment factors indicate that bottom waters at Site 1263 (paleodepth 1500 m) were suboxic before, during, and after the PETM, whereas Site 1262 (3400 m) developed suboxic bottom water conditions during the event [*Chun et al.*, 2010].

The pre-PETM planktonic I/Ca values at Site 1263 (2–3 μmol/mol) are much lower than those at the deeper Site 1262 (~6 μmol/mol) (Figure 3), although the sites were geographically close, so that there probably was no large difference in productivity. Surface water iodate concentrations ranging from 0.05 to 0.35 uM were reported within a small region during a modern hypoxic event in the southern Benguela system [*Truesdale and Bailey*, 2000]. Although the oceanographic setting for Walvis Ridge is not identical to the setting for this modern event, highly dynamic I/Ca spatial variability in nearby sites is not impossible.

The difference in I/Ca is thus probably caused by the presence of a shallow OMZ over Site 1263 throughout the studied period, as supported by the low I/Ca values, the negative D-M values, and the modeling results (Figures 3, 4, and 7). The D-M values at Site 1263 dropped rapidly before the onset of CIE and then increased gradually in the first 100 kyr of the event. This trend is mainly driven by the changes in I/Ca values of the deep dwellers and not the relatively stable I/Ca values in the mixed-layer genera (Figure 3). The period of intensified deoxygenation, as indicated by lower I/Ca, appears to have been relatively short ($<$100 kyr) at 1263, as compared to other open ocean sites (Figure 3).

A possible scenario at Site 1263 is that the upper ocean iodate concentration was lowered by the shoaling of an OMZ during the PETM and that migration of *Subbotina* species could not compensate for the iodate gradient change. We thus conclude that the OMZ in the Walvis Ridge region (Site 1263) may have expanded vertically, both upward and downward, as indicated by I/Ca and Mn data [*Chun et al.*, 2010].

The upward extension of OMZs might have been widespread, influencing pelagic ecosystems [*John et al.*, 2013]. Such a trajectory was predicted for the future [*Stramma et al.*, 2012], contributing to the different composition of pelagic ecosystems during Greenhouse climates [*Norris et al.*, 2013]. A vertical compression of the zone above the OMZ thus may also have been one of the drivers for the observed changes in planktonic foraminiferal assemblages during hyperthermal events, commonly attributed to changes in ocean stratification [*Kelly et al.*, 1998; *Kelly*, 2002; *Petrizzo*, 2007; *Stap et al.*, 2010]. In addition, the enrichment in fish debris in sediment above the base of the CIE at Shatsky Rise sites [*Colosimo et al.*, 2006] could reflect a mortality event due to expansion of the OMZ, rather than due to carbonate dissolution, with % fish debris not precisely correlated with $\%CaCO_3$.

Methane oxidation was proposed as one of the major causes of low-oxygen conditions at intermediate depth such as the New Zealand margin [*Nicolo et al.*, 2010]. This current data set does not shed new light on a potential role of methane as a cause of ocean deoxygenation during the PETM, because we focus on the open ocean conditions rather than on continental margin locations. The rapid release of methane and other hydrocarbon during the Deepwater Horizon oil spill in the Gulf of Mexico in 2010 did result in minor O_2 depletion, but the low-O_2 anomaly did not propagate to the upper ocean [*Kessler et al.*, 2011]. This event differs from the PETM in many aspects but could be seen as indicative that the upper water column in open ocean settings could escape deoxygenation related to methane oxidation. The observation that deoxygenation may have been more severe in Atlantic and Indian Oceans, however, might suggest that hydrate dissociation could have been a causal factor in these more enclosed basins, but not in the much larger Pacific Ocean.

5.5. Shell Recrystallization

Planktonic foraminifera in carbonate-rich pelagic sections usually undergo recrystallization within the upper sediment column. Pore waters deeper than a few centimeters below seafloor do not contain iodate but only contain iodide [*Kennedy and Elderfield*, 1987] which cannot be incorporated in the carbonate structure

[*Lu et al.*, 2010]. Recrystallization in pore waters thus would lower the I/Ca values. We argue that such diagenetic loss of carbonate iodate probably would not interfere with the observed trends. Recrystallization typically is less important in benthic and deep-dwelling planktonics than in mixed-layer species. If recrystallization had impacted the I/Ca records, the D-M values would have increased, incorrectly indicating oxygenated water masses. Specifically, relatively low I/Ca values combined with positive D-M values would be suspicious. The two data points at Site 690 very close to the onset of CIE may be an example, although 690 is generally considered to have well-preserved tests. Recrystallization is known for Site 865 [*Kozdon et al.*, 2013], but the I/Ca values are the highest among all sites, indicating that the proxy may not be very susceptible to diagenetic alteration.

5.6. Depth Habitat

The discussions about I/Ca and D-M values are based on the assumption that there was no major shift in habitat of planktonic foraminifera. This assumption may not hold for PETM, given the warming and increased stratification. Specifically, *Kelly et al.* [1996, 1998, 2005] describe significant changes in the foraminifer assemblages at Sites 865 and 690, including the appearance of warm water taxa such as *Morozovella* at high latitudes, and shifts in the relative abundances of species of *Acarinina*. The mixed-layer genera, taxa, however, contain photosymbionts and thus would not be expected to migrate below the zone where light penetrates, thus keeping a vertical distance from the thermocline calcifiers (see also discussion in *Penman et al*. [2014]). The deep-dwellers could have adjusted to warming by migrating to deeper levels, whereas the expansion of OMZ likely limited such downward migration. Indeed, an abrupt decrease in abundance or absence of the deep-dwelling *Subbotina* during the peak CIE is observed at many localities [*Kelly et al.*, 1998; *Arenillas et al.*, 1999; *Kelly et al*., 2005; *Luciani et al*., 2007; *Petrizzo*, 2007] and thus might have been caused by loss of deeper habitat space. At this moment we cannot evaluate the influence of habitat change on the interpretation of I/Ca records in detail, especially the temporal trends in D-M values. Higher-resolution records combined with faunal assemblage analyses are needed to fully evaluate this topic and could provide new light on the question of planktonic depth migration during climate change.

5.7. Symbiont Bearing Planktonic Foraminifera

Active photosymbionts could increase the iodate concentration in the direct microenvironment of calcification of the test, but we do not have information on the magnitude of such an effect from culture studies. A potential loss of photosymbionts, as argued for the Middle Eocene Climate Optimum [*Edgar et al.*, 2013], could have caused a decline in I/Ca in species that carried photosymbionts. If that had been the only cause of the I/Ca decline at the onset of the PETM, the decline would have been seen in mixed-layer dwellers only, in contrast to observations (Figure 3). At Site 690, the decline in I/Ca in M species was somewhat larger than that in D species (Figure 3), so a loss of photosymbionts might have contributed to the I/Ca decline, specifically for the two samples with maximum D-M (Figure 4).

5.8. Whole-Ocean Change in Iodine

The decline in I/Ca could potentially have been caused by a decline in total iodine concentration in seawater, but there is no evidence for globally high organic burial rates [*Paytan et al.*, 2007], which would be the main sink for iodine. The iodine content of foraminifera from organic-rich sections across the PETM, however, should be investigated to further constrain the burial flux. The pore water iodine concentration is typically up to 3 orders of magnitude higher than the seawater iodine concentration in modern methane hydrate fields [*Lu et al.*, 2008], and the destabilization of hydrate might have released sedimentary pore water iodine into the ocean, slightly increasing (rather than decreasing) the total iodine concentration in seawater. If this had occurred, we would have underestimated the degree of deoxygenation.

6. Conclusions

Our records demonstrate that foraminiferal I/Ca may be a useful paleoceanographic proxy for changes in oxygenation in the upper ocean, tracing the horizontal and vertical extent of OMZs. The difference between the I/Ca of mixed-layer and deeper-dwelling planktonic foraminifera can provide insight into the evolution of the OMZ at a site, and our I/Ca records demonstrate that OMZs expanded during the PETM. This proxy thus has promise for reconstructing paleodeoxygenation at various depths in the water column under oxic/suboxic conditions, complementing the use of bulk sediment proxies (e.g., Mn and Mo) and organic biomarkers (e.g., isorenieretane) for anoxic/euxinic conditions.

Acknowledgments
This work is supported by NSF OCE 1232620 to Lu and NSF OCE 1232413 to Thomas. Thomas and Rickaby also thank the Leverhulme Trust (UK). All model simulations were done on NCAR computers, supported by NSF. Data can be found in the supporting information. Two anonymous reviewers helped to improve the manuscript greatly.

References

Akhmet'ev, M. A., N. I. Zaporozhets, A. I. Iakovleva, G. N. Aleksandrova, V. N. Beniamovsky, T. V. Oreshkina, Z. N. Gnibidenko, and Z. A. Dolya (2010), Comparative analysis of marine paleogene sections and biota from West Siberia and the Arctic Region, *Stratigr. Geol. Correl.*, *18*(6), 635–659.

Alegret, L., S. Ortiz, and E. Molina (2009), Extinction and recovery of benthic foraminifera across the Paleocene-Eocene Thermal Maximum at the Alamedilla section (Southern Spain), *Palaeogeogr. Palaeoclimatol. Palaeoecol.*, *279*(3-4), 186–200.

Alegret, L., S. Ortiz, I. Arenillas, and E. Molina (2010), What happens when the ocean is overheated? The foraminiferal response across the Paleocene-Eocene Thermal Maximum at the Alamedilla section (Spain), *Geol. Soc. Am. Bull.*, *122*(9-10), 1616–1624.

Algeo, T. J., and T. W. Lyons (2006), Mo-total organic carbon covariation in modern anoxic marine environments: Implications for analysis of paleoredox and paleohydrographic conditions, *Paleoceanography*, *21*, PA1016, doi:10.1029/2004PA001112.

Anbar, A. D., and G. W. Gordon (2008), Redox renaissance, *Geology*, *36*(3), 271–272.

Arenillas, I., E. Molina, and B. Schmitz (1999), Planktic foraminiferal and ^{13}C isotopic changes across the Paleocene/ Eocene boundary at Possagno (Italy), *Int. J. Earth Sci.*, *88*(2), 352–364.

Bains, S., R. M. Corfield, and R. D. Norris (1999), Mechanisms of climate warming at the end of the Paleocene, *Science*, *285* (2048), 724–727.

Barker, S., M. Greaves, and H. Elderfield (2003), A study of cleaning procedures used for foraminiferal Mg/Ca paleothermometry, *Geochem. Geophys. Geosyst.*, *4*(9), 8407, doi:10.1029/2003GC000559.

Bluhm, K., P. L. Croot, O. Huhn, G. Rohardt, and K. Lochte (2011), Distribution of iodide and iodate in the Atlantic sector of the southern ocean during austral summer, *Deep Sea Res., Part II*, *58*(25-26), 2733–2748.

Boersma, A., I. Premoli-Silva, and P. Hallock (1998), *Trophic Models for the Well-Mixed Warm Oceans Across the Paleocene/Eocene Epoch Boundary*, Columbia Univ. Press, New York.

Bograd, S. J., C. G. Castro, E. Di Lorenzo, D. M. Palacios, H. Bailey, W. Gilly, and F. P. Chavez (2008), Oxygen declines and the shoaling of the hypoxic boundary in the California Current, *Geophys. Res. Lett.*, *35*, L12607, doi:10.1029/2008GL034185.

Boyle, E. A., and L. D. Keigwin (1985), Comparison of Atlantic and Pacific paleochemical records for the last 215,000 years—Changes in deep ocean circulation and chemical inventories, *Earth Planet. Sci. Lett.*, *76*(1-2), 135–150.

Bralower, T. J. (2002), Evidence of surface water oligotrophy during the Paleocene-Eocene thermal maximum: Nannofossil assemblage data from Ocean Drilling Program Site 690, Maud Rise, Weddell Sea, *Paleoceanography*, *17*(2), 1023, doi:10.1029/2001PA000662.

Bralower, T. J., J. C. Zachos, E. Thomas, M. Parrow, C. K. Paull, D. C. Kelly, I. P. Silva, W. V. Sliter, and K. C. Lohmann (1995), Late Paleocene to Eocene paleoceanography of the equatorial Pacific Ocean—Stable isotopes recorded at Ocean Drilling Program Site-865, Allison Guyot, *Paleoceanography*, *10*(4), 841–865, doi:10.1029/95PA01143.

Bralower, T. J., D. C. Kelly, and D. J. Thomas (2004), Comment on "Coccolith Sr/Ca records of productivity during the Paleocene-Eocene thermal maximum from the Weddell Sea" by Heather M. Stoll and Santo Bains, *Paleoceanography*, *19*, PA1014, doi:10.1029/2003PA000953.

Campos, M., A. M. Farrenkopf, T. D. Jickells, and G. W. Luther (1996), A comparison of dissolved iodine cycling at the Bermuda Atlantic time-series station and Hawaii Ocean time-series station, *Deep Sea Res., Part II*, *43*(2-3), 455–466.

Campos, M., R. Sanders, and T. Jickells (1999), The dissolved iodate and iodide distribution in the South Atlantic from the Weddell Sea to Brazil, *Mar. Chem.*, *65*(3-4), 167–175.

Chance, R., et al. (2010), Seasonal and interannual variation of dissolved iodine speciation at a coastal Antarctic site, *Mar. Chem.*, *118*(3–4), 171–181.

Chun, C. O. J., M. L. Delaney, and J. C. Zachos (2010), Paleoredox changes across the Paleocene-Eocene thermal maximum, Walvis Ridge (ODP Sites 1262, 1263, and 1266): Evidence from Mn and U enrichment factors, *Paleoceanography*, *25*, PA4202, doi:10.1029/2009PA001861.

Colosimo, A. B., T. J. Bralower, and J. C. Zachos (2006), Evidence for lysocline shoaling at the Paleocene/Eocene Thermal Maximum on Shatsky Rise, Northwest Pacific, in *Proc. Ocean Drill. Program Part B Sci. Results*, vol. 198, edited by T. J. Bralower, I. Premoli Silva, and M. J. Malone, pp. 1–36, College Station, Tex., doi:10.2973/odp.proc.sr.198.112.2006.

Dickson, A. J., A. S. Cohen, and A. L. Coe (2012), Seawater oxygenation during the Paleocene-Eocene Thermal Maximum, *Geology*, *40*(7), 639–642.

Dickson, A. J., R. L. Rees-Owen, C. März, A. L. Coe, A. S. Cohen, R. D. Pancost, K. Taylor, and E. Shcherbinina (2014), The spread of marine anoxia on the northern Tethys margin during the Paleocene-Eocene Thermal Maximum, *Paleoceanography*, *29*, 471–488, doi:10.1002/2014PA002629.

Doney, S. C., K. Lindsay, I. Fung, and J. John (2006), Natural variability in a stable, 1000-yr global coupled climate-carbon cycle simulation, *J. Clim.*, *19*(13), 3033–3054.

Dunkley Jones, T., D. J. Lunt, D. N. Schmidt, A. Ridgwell, A. Sluijs, P. J. Valdes, and M. Maslin (2013), Climate model and proxy data constraints on ocean warming across the Paleocene–Eocene Thermal Maximum, *Earth Sci. Rev.*, *125*, 123–145.

Edgar, K. M., S. M. Bohaty, S. J. Gibbs, P. F. Sexton, R. D. Norris, and P. A. Wilson (2013), Symbiont 'bleaching' in planktonic foraminifera during the Middle Eocene Climatic Optimum, *Geology*, *41*(1), 15–18.

Ezard, T. H. G., T. Aze, P. N. Pearson, and A. Purvis (2011), Interplay between changing climate and species' ecology drives macroevolutionary dynamics, *Science*, *332*(6027), 349–351.

Falkowski, P. G., et al. (2011), Ocean deoxygenation: Past, present and future, *Eos Trans. AGU*, *92*, 409–410, doi:10.1029/2011EO460001.

Farrenkopf, A. M., and G. W. Luther (2002), Iodine chemistry reflects productivity and denitrification in the Arabian Sea: Evidence for flux of dissolved species from sediments of western India into the OMZ, *Deep Sea Res., Part II*, *49*(12), 2303–2318.

Gavrilov, Y. O., L. A. Kodina, I. Y. Lubchenko, and N. G. Muzylev (1997), The late Paleocene anoxic event in epicontinental seas of peri-Tethys and formation of the sapropelite unit: Sedimentology and geochemistry, *Lithol. Min. Resour.*, *32*(5), 427–450.

Gibbs, S. J., T. J. Bralower, P. R. Bown, J. C. Zachos, and L. M. Bybell (2006), Shelf and open-ocean calcareous phytoplankton assemblages across the Paleocene-Eocene Thermal Maximum: Implications for global productivity gradients, *Geology*, *34*(4), 233–236.

Gibbs, S. J., H. M. Stoll, P. R. Bown, and T. J. Bralower (2010), Ocean acidification and surface water carbonate production across the Paleocene-Eocene thermal maximum, *Earth Planet. Sci. Lett.*, *295*(3-4), 583–592.

Gilly, W. F., J. M. Beman, S. Y. Litvin, and B. H. Robison (2013), Oceanographic and biological effects of shoaling of the oxygen minimum zone, in *Annual Review of Marine Science*, vol. 5, edited by C. A. Carlson and S. J. Giovannoni, pp. 393–420, Annual Reviews, Palo Alto, Calif.

Gooday, A. J., B. J. Bett, E. Escobar, B. Ingole, L. A. Levin, C. Neira, A. V. Raman, and J. Sellanes (2010), Habitat heterogeneity and its influence on benthic biodiversity in oxygen minimum zones, *Mar. Ecol.*, *31*(1), 125–147.

Hallock, P. (1987), Fluctuations in the trophic resource continuum: A factor in global diversity cycles?, *Paleoceanography*, *2*(5), 457–471, doi:10.1029/PA002i005p00457.

Hardisty, D. S., Z. Lu, N. Planavsky, A. Bekker, P. Philippot, X. Zhou, and T. W. Lyons (2014), An iodine record of Paleoproterozoic surface ocean oxygenation, *Geology*, doi:10.1130/G35439.1.

Helm, K. P., N. L. Bindoff, and J. A. Church (2011), Observed decreases in oxygen content of the global ocean, *Geophys. Res. Lett.*, *38*, L23602, doi:10.1029/2011GL049513.

Hoenisch, B., et al. (2012), The geological record of ocean acidification, *Science*, *335*(6072), 1058–1063.
Jenkyns, H. C. (2010), Geochemistry of oceanic anoxic events, *Geochem. Geophys. Geosyst.*, *11*, Q03004, doi:10.1029/2009GC002788.
Jiang, S. J., and S. W. Wise (2009), Distinguishing the influence of diagenesis on the paleoecological reconstruction of nannoplankton across the Paleocene/Eocene Thermal Maximum: An example from the Kerguelen Plateau, southern Indian Ocean, *Mar. Micropaleontol.*, *72*(1–2), 49–59.
Jickells, T. D., S. S. Boyd, and A. H. Knap (1988), Iodine cycling in the Sargasso Sea and the Bermuda inshore waters, *Mar. Chem.*, *24*(1), 61–82.
John, E. H., P. N. Pearson, H. K. Coxall, H. Birch, B. S. Wade, and G. L. Foster (2013), Warm ocean processes and carbon cycling in the Eocene, *Philos. Trans. R. Soc. A*, *371*(2001), 20130099.
Keeling, R. F., A. Kortzinger, and N. Gruber (2010), Ocean deoxygenation in a warming world, *Annu. Rev. Mar. Sci.*, *2*, 199–229.
Kelly, D. C. (2002), Response of Antarctic (ODP Site 690) planktonic foraminifera to the Paleocene-Eocene thermal maximum: Faunal evidence for ocean/climate change, *Paleoceanography*, *17*(4), 1071, doi:10.1029/2002PA000761.
Kelly, D. C., T. J. Bralower, J. C. Zachos, I. P. Silva, and E. Thomas (1996), Rapid diversification of planktonic foraminifera in the tropical Pacific (ODP Site 865) during the late Paleocene thermal maximum, *Geology*, *24*(5), 423–426.
Kelly, D. C., T. J. Bralower, and J. C. Zachos (1998), Evolutionary consequences of the latest Paleocene thermal maximum for tropical planktonic foraminifera, *Palaeogeogr. Palaeoclimatol. Palaeoecol.*, *141*(1-2), 139–161.
Kelly, D. C., J. C. Zachos, T. J. Bralower, and S. A. Schellenberg (2005), Enhanced terrestrial weathering/runoff and surface ocean carbonate production during the recovery stages of the Paleocene-Eocene Thermal Maximum, *Paleoceanography*, *20*, PA4023, doi:10.1029/2005PA001163.
Kennedy, H. A., and H. Elderfield (1987), Iodine diagenesis in pelagic deep-sea sediments, *Geochim. Cosmochim. Acta*, *51*(9), 2489–2504.
Kessler, J. D., et al. (2011), A persistent oxygen anomaly reveals the fate of spilled methane in the deep Gulf of Mexico, *Science*, *331*(6015), 312–315.
Koopmans, M. P., J. Koster, H. M. E. vanKaamPeters, F. Kenig, S. Schouten, W. A. Hartgers, J. W. deLeeuw, and J. S. S. Damste (1996), Diagenetic and catagenetic products of isorenieratene: Molecular indicators for photic zone anoxia, *Geochim. Cosmochim. Acta*, *60*(22), 4467–4496.
Kozdon, R., D. C. Kelly, K. Kitajima, A. Strickland, J. H. Fournelle, and J. W. Valley (2013), In situ delta O-18 and Mg/Ca analyses of diagenetic and planktonic foraminiferal calcite preserved in a deep-sea record of the Paleocene-Eocene thermal maximum, *Paleoceanography*, *28*, 517–528, doi:10.1002/palo.20048.
Kuepper, F. C., et al. (2011), Commemorating two centuries of iodine research: An interdisciplinary overview of current research, *Angew. Chem. Int. Ed.*, *50*(49), 11,598–11,620.
Larrasoana, J. C., A. P. Roberts, L. Chang, S. A. Schellenberg, J. FitzGerald, R. D. Norris, and J. C. Zachos (2012), Magnetotactic bacterial response to Antarctic dust supply during the Palaeocene-Eocene Thermal Maximum, *Earth Planet. Sci. Lett.*, *333–334*, 122–133.
Levin, L. A. (2003), Oxygen minimum zone benthos: Adaptation and community response to hypoxia, *Oceanogr. Mar. Biol.*, *41*, 1–45.
Lu, Z., C. Hensen, U. Fehn, and K. Wallmann (2008), Halogen and 129I systematics in gas hydrate fields at the northern Cascadia margin (IODP Expedition 311): Insights from numerical modeling, *Geochem. Geophys. Geosyst.*, *9*, Q10006, doi:10.1029/2008GC002156.
Lu, Z., H. C. Jenkyns, and R. E. M. Rickaby (2010), Iodine to calcium ratios in marine carbonate as a paleo-redox proxy during oceanic anoxic events, *Geology*, *38*(12), 1107–1110.
Luciani, V., L. Giusberti, C. Agnini, J. Backman, E. Fornaciari, and D. Rio (2007), The Paleocene-Eocene Thermal Maximum as recorded by Tethyan planktonic formaminifera in the Forada section (northern Italy), *Mar. Micropaleontol.*, *64*(3–4), 189–214.
Ma, Z., E. Gray, E. Thomas, B. Murphy, J. C. Zachos, and A. Paytan (2014), Carbon sequestration during the Paleocene Eocene Thermal Maximum by an efficient biological pump, *Nat. Geosci.*, *7*, 382–388.
McInerney, F. A., and S. L. Wing (2011), The Paleocene-Eocene Thermal Maximum: A perturbation of carbon cycle, climate, and biosphere with implications for the future, in *Annual Review of Earth and Planetary Sciences*, vol. 39, edited by R. Jeanloz and K. H. Freeman, pp. 489–516, Annual Reviews, Palo Alto, Calif.
McNeil, D. H., M. G. Parsons, and J. Russel-Houston (2013), The Paleocene-Eocene thermal maximum in the Arctic Beaufort–Mackenzie Basin—Palynomorphs, carbon isotopes and benthic foraminiferal turnover, *Bull. Can. Pet. Geol.*, *61*(2), 157–186.
Moran, K., et al. (2006), The Cenozoic palaeoenvironment of the Arctic Ocean, *Nature*, *441*(7093), 601–605.
Nagy, J., D. Jargvoll, H. Dypvik, M. Jochmann, and L. Riber (2013), Environmental changes during the Paleocene-Eocene Thermal Maximum in Spitsbergen as reflected by benthic foraminifera, *Polar Res.*, *32*, 19737.
Nguyen, T. M. P., M. R. Petrizzo, and R. P. Speijer (2009), Experimental dissolution of a fossil foraminiferal assemblage (Paleocene-Eocene Thermal Maximum, Dababiya, Egypt): Implications for paleoenvironmental reconstructions, *Mar. Micropaleontol.*, *73*(3-4), 241–258.
Nicolo, M. J., G. R. Dickens, and C. J. Hollis (2010), South Pacific intermediate water oxygen depletion at the onset of the Paleocene-Eocene thermal maximum as depicted in New Zealand margin sections, *Paleoceanography*, *25*, PA4210, doi:10.1029/2009PA001904.
Norris, R. D., S. K. Turner, P. M. Hull, and A. Ridgwell (2013), Marine ecosystem responses to Cenozoic global change, *Science*, *341*(6145), 492–498.
Paelike, C., M. L. Delaney, and J. Zachos (2014), Deep-sea redox across the Paleocene-Eocene thermal maximum, *Geochem. Geophys. Geosyst.*, *15*, 1038–1053, doi:10.1002/2013GC005074.
Paytan, A., K. Averyt, K. Faul, E. Gray, and E. Thomas (2007), Barite accumulation, ocean productivity, and Sr/Ba in barite across the Paleocene-Eocene Thermal Maximum, *Geology*, *35*(12), 1139–1142.
Penman, D. E., B. Hönisch, R. E. Zeebe, E. Thomas, and J. C. Zachos (2014), Rapid and sustained surface ocean acidification during the Paleocene-Eocene Thermal Maximum, *Paleoceanography*, *29*, 357–369, doi:10.1002/2014PA002621.
Petrizzo, M. R. (2007), The onset of the Paleocene-Eocene Thermal Maximum (PETM) at Sites 1209 and 1210 (Shatsky Rise, Pacific Ocean) as recorded by planktonic foraminifera, *Mar. Micropaleontol.*, *63*(3-4), 187–200.
Ravizza, G., R. N. Norris, J. Blusztajn, and M. P. Aubry (2001), An osmium isotope excursion associated with the late Paleocene thermal maximum: Evidence of intensified chemical weathering, *Paleoceanography*, *16*(2), 155–163, doi:10.1029/2000PA000541.
Reid, P. C., et al. (2009), Impacts of the oceans on climate change, in *Advances in Marine Biology*, vol. 56, edited by D. W. Sims, pp. 1–150, Elsevier Acad. Press Inc., San Diego, Calif.
Röhl, U., T. Westerhold, T. J. Bralower, and J. C. Zachos (2007), On the duration of the Paleocene-Eocene thermal maximum (PETM), *Geochem. Geophys. Geosyst.*, *8*, Q12002, doi:10.1029/2007GC001784.
Rue, E. L., G. J. Smith, G. A. Cutter, and K. W. Bruland (1997), The response of trace element redox couples to suboxic conditions in the water column, *Deep Sea Res., Part I*, *44*(1), 113–134.
Sluijs, A., et al. (2006), Subtropical arctic ocean temperatures during the Palaeocene/Eocene thermal maximum, *Nature*, *441*(7093), 610–613.
Smith, J. D., E. C. V. Butler, D. Airey, and G. Sandars (1990), Chemical-properties of a low-oxygen water column in port-hacking (Australia)—Arsenic, iodine and nutrients, *Mar. Chem.*, *28*(4), 353–364.
Speijer, R. P., and T. Wagner (2002), Sea-level changes and black shales associated with the late Paleocene thermal maximum (LPTM): Organic geochemical and micropaleontologic evidence from the southern Tethyam margin (Egypt-Israel), in *Catastrophic Events and Mass Extinctions: Impacts and Beyond*, edited by C. Koeberl and K. MacLeod, *Geol. Soc. Am. Spec. Pap.*, *356*, 533–549.

Stap, L., L. J. Lourens, E. Thomas, A. Sluijs, S. Bohaty, and J. C. Zachos (2010), High-resolution deep-sea carbon and oxygen isotope records of Eocene Thermal Maximum 2 and H2, *Geology*, *38*(7), 607–610.
Stassen, P., E. Thomas, and R. P. Speijer (2012), Integrated stratigraphy of the Paleocene-Eocene thermal maximum in the New Jersey Coastal Plain: Toward understanding the effects of global warming in a shelf environment, *Paleoceanography*, *27*, PA4210, doi:10.1029/2012PA002323.
Stein, R., B. Boucsein, and H. Meyer (2006), Anoxia and high primary production in the Paleogene central Arctic Ocean: First detailed records from Lomonosov Ridge, *Geophys. Res. Lett.*, *33*, L18606, doi:10.1029/2006GL026776.
Stoll, H. M., and S. Bains (2003), Coccolith Sr/Ca records of productivity during the Paleocene-Eocene thermal maximum from the Weddell Sea, *Paleoceanography*, *18*(2), 1049, doi:10.1029/2002PA000875.
Stoll, H. M., N. Shimizu, D. Archer, and P. Ziveri (2007), Coccolithophore productivity response to greenhouse event of the Paleocene-Eocene Thermal Maximum, *Earth Planet. Sci. Lett.*, *258*(1-2), 192–206.
Stramma, L., E. D. Prince, S. Schmidtko, J. Luo, J. P. Hoolihan, M. Visbeck, D. W. R. Wallace, P. Brandt, and A. Koertzinger (2012), Expansion of oxygen minimum zones may reduce available habitat for tropical pelagic fishes, *Nat. Clim. Change*, *2*(1), 33–37.
Summons, R. E., and T. G. Powell (1987), Identification of aryl isoprenoids in source rocks and crude oils—Biological markers for the green sulfur bacteria, *Geochim. Cosmochim. Acta*, *51*(3), 557–566.
Thomas, E. (2007), Cenozoic mass extinctions in the deep sea: What disturbs the largest habitat on Earth?, in *Large Ecosystem Perturbations: Causes and Consequences*, edited by S. Monechi, R. Coccioni, and M. Rampino, *Geol. Soc. Am. Spec. Pap.*, *424*, 1–24.
Thomas, E., N. J. Shackleton, and M. A. Hall (1992), Data report: Carbon isotope stratigraphy of Paleogene bulk sediments, Hole 762C (Exmouth Plateau, eastern Indian Ocean), in *Proc. Ocean Drill. Program Part B Sci. Results*, vol. 122, edited by U. von Rad et al., pp. 897–901, College Station, Tex., doi:10.2973/odp.proc.sr.122.195.1992.
Tian, R. C., J. C. Marty, E. Nicolas, J. Chiaverini, D. RuizPino, and M. D. Pizay (1996), Iodine speciation: A potential indicator to evaluate new production versus regenerated production, *Deep Sea Res., Part I*, *43*(5), 723–738.
Truesdale, V. W., and G. W. Bailey (2000), Dissolved iodate and total iodine during an extreme hypoxic event in the Southern Benguela system, *Estuarine Coastal Shelf Sci.*, *50*(6), 751–760.
Truesdale, V. W., and G. W. Bailey (2002), Iodine distribution in the Southern Benguela system during an upwelling episode, *Cont. Shelf Res.*, *22*(1), 39–49.
Whitney, F. A., H. J. Freeland, and M. Robert (2007), Persistently declining oxygen levels in the interior waters of the eastern subarctic Pacific, *Prog. Oceanogr.*, *75*(2), 179–199.
Wieczorek, R., M. S. Fantle, L. R. Kump, and G. Ravizza (2013), Geochemical evidence for volcanic activity prior to and enhanced terrestrial weathering during the Paleocene Eocene Thermal Maximum, *Geochim. Cosmochim. Acta*, *119*, 391–410.
Winguth, A. M. E., E. Thomas, and C. Winguth (2012), Global decline in ocean ventilation, oxygenation, and productivity during the Paleocene-Eocene Thermal Maximum: Implications for the benthic extinction, *Geology*, *40*(3), 263–266.
Wong, G. T. F., and P. G. Brewer (1977), Marine chemistry of iodine in anoxic basins, *Geochim. Cosmochim. Acta*, *41*(1), 151–159.
Zachos, J. C., et al. (2005), Rapid acidification of the ocean during the Paleocene-Eocene thermal maximum, *Science*, *308*(5728), 1611–1615.